Struct Multidisc Optim (2008) 36:443–456
DOI 10.1007/s00158-007-0201-8

RESEARCH PAPER

Optimization of scattering resonances

P. Heider · D. Berebichez · R. V. Kohn · M. I. Weinstein

Received: 15 August 2007 / Accepted: 9 October 2007 / Published online: 20 February 2008
© Springer-Verlag 2008

Abstract The increasing use of micro- and nano-scale components in optical, electrical, and mechanical systems makes the understanding of loss mechanisms and their quantification issues of fundamental importance. In many situations, performance-limiting loss is due to scattering and radiation of waves into the surrounding structure. In this paper, we study the problem of systematically improving a structure by altering its design so as to decrease the loss. We use sensitivity analysis and local gradient optimization, applied to the scattering resonance problem, to reduce the loss within the class of piecewise constant structures. For a class of optimization problems where the material parameters are constrained by upper and lower bounds, it is observed that an optimal structure is piecewise constant with values achieving the bounds.

Keywords Scattering resonance · Quality factor · Sensitivity analysis

This work was supported in part by the Humboldt Stiftung (PH), NSF-GOALI grant DMS-0313890 (DB, RVK, MIW), NSF grant DMS-0313744 (RVK), and NSF grants DMS-0412305 and DMS-0707850 (MIW).

P. Heider
Mathematisches Institut der Universität zu Köln,
50931 Köln, Germany
e-mail: pheider@math.uni-koeln.de

P. Heider · D. Berebichez · M. I. Weinstein
Department of Applied Physics and Applied Mathematics,
Columbia University, New York, NY, USA

D. Berebichez
e-mail: debbieb@gmail.com

M. I. Weinstein
e-mail: miw2103@columbia.edu

D. Berebichez · R. V. Kohn (✉)
Courant Institute of Mathematical Sciences,
New York University, New York, NY, USA
e-mail: kohn@courant.nyu.edu

1 Introduction and outline

There is great current interest in the design of micro- and nano-structures in dielectric materials for storage, channeling, amplification, compression, filtering, or, in general, manipulation of light pulses. Such structures have a broad range of applications from optical communication technologies to quantum information science. Energy loss is a performance-limiting concern in the design of micro- and nano-scale components. Thus, the question of how to design such components with very low radiative loss is a fundamental question. Periodic structures are important classes of structures (Joannopoulos et al. 1995). In practice, these *photonic crystals* (PCs) are structures with piecewise constant material properties. The ability of these structures to influence light propagation is achieved through variation of the period, the choice of material contrasts, and through the introduction of defects.

We study the problem of scattering loss from a PC with defects, for a class of one-dimensional wave equations:

$$n^2(x)\,\partial_t^2\psi(x,t) \;=\; \partial_x\sigma(x)\partial_x\psi(x,t) \tag{1}$$

The functions $n(x)$ and $\sigma(x)$ are strictly positive, assumed to be variable within some compact set, contained in a bounded open interval, $a < x < b$, and constant outside of it. Without loss of generality, we

assume $\sigma(x) = n(x) = 1$ for $x < a$ and $x > b$. This corresponds to a normalization of the wave speed $c = 1$ in the uniform medium. The region where these functions vary with x is also referred to as the *cavity*. As the wave equation (1) has real-valued and time-independent coefficients, it models a system which conserves energy. Therefore, by cavity loss, we mean *scattering loss*; that is, loss due to leakage of energy from the cavity. This is in contrast to loss due to processes such as material absorption.

Energy leakage or scattering loss from the cavity is governed by the *scattering resonances* associated with the cavity. Scattering resonances are solutions to the eigenvalue equation satisfied by time-harmonic solutions of (1) subject to outgoing radiation conditions, imposed outside the cavity:

The scattering resonance problem (SRP) Seek nontrivial $u(x; k)$, such that

$$\partial_x \sigma(x) \partial_x u(x) + k^2 n^2(x) u(x) = 0, \tag{2}$$

$$(\partial_x + ik)\, u = 0, \quad x = a$$

$$(\partial_x - ik)\, u = 0, \quad x = b \tag{3}$$

At a jump discontinuity, ξ, of $\sigma(x)$ or $n(x)$, (2) is interpreted via the flux continuity relation, obtained by integration across the discontinuity:

$$\sigma(\xi^+)\partial_x u(\xi^+) = \sigma(\xi^-)\partial_x u(\xi^-), \tag{4}$$

where $F(\xi^\pm) = \lim_{\delta \downarrow 0} F(\xi \pm \delta)$. Corresponding to a solution, $u(x, k)$ of **SRP** is an outgoing time-dependent solution $\psi(x, t) = e^{-i\omega t} u(x; k)$, $\omega = ck = k$.

Remark 1 The above one-dimensional **SRP** governs scattering resonances of *slab* type structures. It is a consequence of Maxwell's equations, under the assumption of time-harmonic solutions. Variation in $n(x)$ with σ constant corresponds to the case of *TM polarization*; variation in $\sigma(x)$ with n constant corresponds to *TE polarization*.

SRP is a non-self-adjoint boundary value problem having a sequence of *complex* eigenvalues $\{k_j\}$ satisfying $\operatorname{Im} k_j < 0$ and corresponding resonance modes $u(x; k_j)$. The modes $u(x; k_j)$ are *locally* square integrable but not square integrable over all space. Assuming there are no bound states (non-decaying in time, L^2 states), the evolution of an arbitrary initial condition for (1) admits a *resonance expansion* in terms of time-exponentially decaying states of the form $e^{-ick_j t} u(x; k_j)$, where $u(\cdot; k_j) \in L^2_{loc}$. In particular, for any $A > 0$ and compact set K, there exist $\varepsilon(A, K) > 0$ and $\tau(A, K) > 0$, such that for any compactly supported smooth initial conditions $u(x, 0)$ and $\partial_t u(x, 0)$, the solution $u(x, t)$ satisfies:

$$\left\| u(x,t) - \sum_{\{k_m : \operatorname{Im} k_m \geq -A\}} c_m\, e^{-ick_m t}\, u(x; k_m) \right\|_{L^2(K)} = \mathcal{O}(e^{-A(1+\varepsilon)t}), \quad t \geq \tau; \tag{5}$$

see, for example, Tang and Zworski (2000). Therefore, the rate at which energy escapes from the cavity, measured for example by the rate of decay of field energy within the cavity $\left(\int_{\text{cavity}} |u(x,t)|^2 \mathrm{d}x\right)$, is controlled by the resonance, k_*, with largest imaginary part. The time it takes for the energy, associated with a general initial condition, localized in the defect, to radiate away is $\tau_* = (c|\operatorname{Im} k_*|)^{-1}$. In practice, for example, in experiments, initial conditions can be quite spectrally concentrated, and therefore, the observed time-decay rate is determined by the imaginary parts of resonances whose real parts lie near the spectral support of the initial condition.

Results such as the resonance expansion (5) imply that, to understand the dynamics of scattering loss, it suffices to consider the time-independent spectral problem **SRP**.

Our goal is to apply *sensitivity analysis* and local gradient optimization methods to the scattering resonance problem in the class of piecewise constant structures, to systematically decrease a cavity's loss in a particular frequency range. Our measure of cavity loss is the magnitude of the imaginary part of a scattering resonance.

More specifically, we proceed as follows. Starting with a particular scattering resonance, $k(\sigma_0, n_0)$, of a piecewise constant structure $\sigma_0(x), n_0(x)$, we deform the cavity structure, $(\sigma_0, n_0) \to (\sigma_1 = \sigma_0 + \delta\sigma, n_1 = n_0 + \delta n)$, within the class of piecewise constant structures, so as to increase the imaginary part (decrease $|\operatorname{Im} k|$), i.e., $\operatorname{Im} k(\sigma_1, n_1) > \operatorname{Im} k(\sigma_0, n_0)$. That is, we increase the lifetime τ of the mode. In this study, $\delta\sigma$ and δn are chosen in the direction of the gradient of $\operatorname{Im} k(\sigma_0, n_0)$, with respect to the design parameters, which is computed using sensitivity analysis. For each structure, along the constructed sequence of improving structures, the associated scattering resonance is computed via Newton iteration. In some eigenvalue optimization problems, complications arise when eigenvalues coalesce or have multi-dimensional eigenspaces. Such complications cannot arise in our setting because, in one space dimension, our eigenvalue problem (**SRP**) is easily seen to have simple eigenvalues.

Summary We present a study of three classes of optimization problems for **SRP** with $\sigma(x)$, the parameter to be optimized, and $n(x) \equiv 1$:

1. Opt, in which σ is piecewise constant but unconstrained,
2. Opt_{area}, in which σ is piecewise constant with fixed $\int_a^b \sigma(s)\mathrm{d}s$, and
3. Opt_{max}, in which σ is piecewise constant and upper and lower bounds $1 = \sigma_{\min} \leq \sigma(x) \leq \sigma_{\max}$.

Our structures lie in Σ_N, the set of piecewise constant structures $[a, b]$, with at most N jump discontinuities. We first explore all three classes of problems fixing, throughout the optimization, the intervals on which σ is constant. Then, for Opt_{max}, we relax this constraint and allow both the N values of σ and the $N-2$ points of discontinuity to be varied during the optimization. In the latter case, we find (when N is taken large enough) that the optimal structure is one where σ takes on the value $\sigma_{\min}$ or $\sigma_{\max}$ on each subinterval.

Gradient methods have also been applied to achieve better confinement, as measured by, for example, mode-variance (Dobson and Santosa 2004) and energy flux (Lipton et al. 2003). The objective function one chooses to maximize is often called the *Q-factor* or quality factor. In this paper, we apply gradient methods to the more natural measure of confinement, $Q = |\operatorname{Im} k|^{-1}$, the reciprocal imaginary part of the resonance. Kao and Santosa (2007) recently used discretization of an integral equation (in one and two space dimensions) and gradient methods to increase a slightly different quality factor, namely the ratio of real to imaginary parts of k (this measures the loss per cycle of the resonance, viewed as an oscillator). Other, less systematic approaches have been used in the physics literature. One such approach proceeds by first (a) specifying a proposed cavity mode profile, engineered to minimize a physically motivated cost functional, then (b) using the differential equation to solve for the dielectric function (a coefficient in the equation) in terms of the specified mode (Geremia et al. 2002). Optimally localizing the eigenmodes of an inhomogeneous membrane, a self-adjoint analogue of our problem, has been studied in Dobson and Santosa (2004). Another class of self-adjoint problems is the maximization of photonic band gap widths (Burger et al. 2004; Cox and Dobson 1999; Kao et al. 2005; Osher and Santosa 2001; Sigmund and Jensen 2003). We also note that the optimization problems we consider can be viewed in the context of the large class of shape optimization problems associated with elliptic partial differential equations (Pironneau 1984).

Finally, we remark that resonances are *unforced* or *free* modes of a leaky cavity. They can be excited via scattering experiments, in which waves are incident on the cavity from outside. In our simple one-dimensional setting, part of the energy is reflected, and part is transmitted. No energy is trapped because the structure has no bound states, and, as the medium is conservative, there is no loss to material absorbtion. Resonances appear as peaks in the transmission coefficient as a function of wavelength, in wavelength ranges where the transmission is typically low. The real part of a scattering resonance energy corresponds to the location of the transmission peak and the imaginary part, to the transmission peak width (Ramdani and Shipman 2007). Thus, our optimization corresponds to the sharpening of a transmission peak, by modification of the cavity.

1.1 General remarks on periodic or truncated periodic structures, and defects

The above remarks are general, applying to any structure which does not have non-decaying (with time) L^2 bound states. We now discuss the class of structures which motivate this study. Waves in periodic structures, e.g., electromagnetic, acoustic, or elastic, are governed by a wave equation with periodic coefficients. These equations have plane wave type states, parametrized by a continuous spectrum equal to the union of closed intervals called *bands* (photonic pass-bands). The complement of the spectrum (on the real axis) consists of the union of open intervals called *gaps* (photonic band-gaps). Arbitrary spatially localized states can be represented as a generalized Fourier superposition of such states. Furthermore, solutions to the initial value problem for the time-dependent wave equation in a periodic structure disperse to zero with advancing time (Korotyaev 1997; Cuccagna 2007).

A localized defect in a periodic structure gives rise to discrete eigenvalues in the gaps (Figotin and Klein 1998). Thus, a periodic structure with a spatially localized defect may support localized time-periodic (non-decaying) states. In applications, photonic structures are often *truncations* of periodic structures with defects; see Fig. 2, where outside a compact set these structures have constant physical parameters. *This* finite structure no longer has localized eigenstates. Its spectrum is continuous, and, as in the case of the spatially homogeneous wave equation or in the wave equation with globally periodic coefficients, solutions tend to zero as $t \to \infty$ locally on any compact set. As explained above, the manner in which the local energy tends to zero is controlled by the resonance expansion. Note that, as the truncation is removed, certain scattering resonance

frequencies, associated with defect eigenstates of the infinite structure, approach eigenvalues on the real axis and become infinitely long-lived (non-decaying) states.

1.2 Outline

The article is structured as follows. In Section 2, we define Σ_N, the class of admissible piecewise constant structures, with at most N jump discontinuities in $\sigma(x)$ and $n(x)$. Section 3 concerns sensitivity analysis, the computation of variations in a scattering resonance with respect to changes in the design parameters. Section 4 describes two approaches to the computation of scattering resonances: one based on use of the exact solution in each interval where the material properties are constant, the other based on finite differences. Section 5 contains a discussion of numerical optimization results for the three classes of problems discussed above.

2 Admissible piecewise constant structures: the class Σ_N

We shall investigate the scattering resonance problem for a class of piecewise constant structures, which we denote by Σ_N. A schematic diagram of a typical structure is presented in Fig. 1. The set Σ_N consists of piecewise constant structures, $(\sigma(x), n(x))$, which for $j = 2, \ldots, N$, take on the values (σ_j, n_j) on the intervals (x_{j-1}, x_j). The endpoints $x_1 = a$ and $x_N = b$ are fixed as are the values $\sigma(x) = \sigma_1 = \sigma_{N+1} = 1$ and $n(x) = n_1 = n_{N+1} = 1$, for $x < a$ and $x > b$.

$$n(x) = \begin{cases} n_1 = 1 & : \quad x < x_1 = a \\ n_j & : \quad x_{j-1} < x < x_j, \ j = 2, \ldots, N \\ n_{N+1} = 1 & : \quad b = x_N < x \end{cases} . \tag{6}$$

$$\sigma(x) = \begin{cases} \sigma_1 = 1 & : \quad x < a \\ \sigma_j & : \quad x_{j-1} < x < x_j, \ j = 2, \ldots, N \\ \sigma_{N+1} = 1 & : \quad b < x \end{cases} . \tag{7}$$

Thus, a structure $(\sigma(x), n(x)) \in \Sigma_N$ is a pair of piecewise constant functions determined by $3N - 4$ parameters:

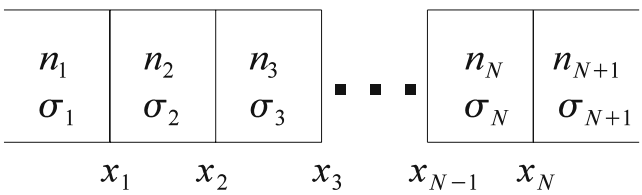

Fig. 1 The functions $\sigma(x)$ and $n(x)$ are step functions. They are assumed to have the value 1 to the left and right of the PC. The jump discontinuities of $\sigma(x)$ and $n(x)$ occur at the points x_j

$N - 2$ interior points of discontinuity: $x_2, \ldots, x_{N-1}$ and $2(N - 1)$ values: σ_j and n_j of $\sigma(x)$ and $n(x)$, respectively, on the intervals (x_{j-1}, x_j), $j = 2, \ldots, N$.

For simplicity, we restrict to structures at which the set of possible points of discontinuity of $\sigma(x)$ and $n(x)$ is the same. Our study can easily be extended to more general structures.

3 Local optimization and sensitivity analysis

As noted in Section 1, $|\mathrm{Im}\, k_{\mathrm{res}}|^{-1}$, $(\mathrm{Im}\, k_{\mathrm{res}} < 0)$ is a measure of the decay rate of the mode or life-time of the mode, $u(x; k_{\mathrm{res}})$.

Optimization problem

Deform the structure, defined by $(\sigma(x), n(x))$*, so as to maximize* $\mathrm{Im}\, k_{\mathrm{res}}$.

In fact, we shall consider several optimization problems:

1. Opt: maximize $\mathrm{Im}\, k_{\mathrm{res}}$ over structures (σ, n), defined on $[a, b]$, with $\sigma(x) = n(x) = 1$ for $x \notin [a, b]$.
2. $\mathrm{Opt}_{\mathrm{area}}$: maximize $\mathrm{Im}\, k_{\mathrm{res}}$ over structures (σ, n), defined on $[a, b]$, with $\sigma(x) = n(x) = 1$ for $x \notin [a, b]$ and $\int_a^b \sigma(y)dy$ fixed.
3. $\mathrm{Opt}_{\mathrm{max}}$: maximize $\mathrm{Im}\, k_{\mathrm{res}}$ over structures (σ, n), defined on $[a, b]$, with $\sigma(x) = n(x) = 1$ for $x \notin [a, b]$, such that $\sigma_{\min} \le \sigma(x) \le \sigma_{\max}$ and $n_{\min} \le n(x) \le n_{\max}$.

The direction of *steepest ascent* of the functional $(\sigma, n) \mapsto \mathrm{Im}\, k_{\mathrm{res}}(\sigma, n)$, is in the direction of the gradient or, in the case of constrained optimization, a projected gradient. Hence, we seek expressions for the gradients of $k_{\mathrm{res}}(\sigma, n)$ with respect to the "design parameters" $\sigma(x)$ and $n(x)$: $\frac{\delta k_{\mathrm{res}}}{\delta \sigma}$ and $\frac{\delta k_{\mathrm{res}}}{\delta n}$, where the total variation of k_{res} is given by[1]:

$$\delta k = \left\langle \frac{\delta k_{\mathrm{res}}}{\delta \sigma}, \ \delta\sigma \right\rangle + \left\langle \frac{\delta k_{\mathrm{res}}}{\delta n}, \ \delta n \right\rangle . \tag{8}$$

The computation of such gradients is also called sensitivity analysis. We first implement sensitivity analysis

[1] We define $\langle f, g \rangle = \int_a^b f(x)g(x)\mathrm{d}x$.

in the setting of general structures and, then, specialize to the discrete setting associated with the class, Σ_N, of piecewise constant structures.

3.1 Sensitivity analysis—general setting

To avoid cumbersome notation, where it causes no confusion, we shall denote a resonance, k_{res}, simply by k. Furthermore, when studying $\delta k_{\text{res}}/\delta\sigma$, we suppress the dependence of k_{res} on $n(x)$, and similarly, we suppress the dependence on $\sigma(x)$, when we study $\delta k_{\text{res}}/\delta n$.

Computation of $\delta k_{\text{res}}/\delta\sigma$ Denote by σ_0 an initial structure and $k(\sigma_0)$, one of its scattering resonance frequencies. Suppose we make a small perturbation in σ, with $n(x) = n_0(x)$ fixed:

$$\sigma_0(x) \longrightarrow \sigma_0(x) + \delta\sigma(x). \tag{9}$$

To compute $\delta k_{\text{res}}/\delta\sigma$, we expand the scattering resonance for the structure $\sigma_0 + \delta\sigma$ about the scattering resonance for the structure, σ_0:

$$\begin{aligned} \sigma &= \sigma_0 + \delta\sigma \\ u(x;\sigma) &= u_0(x) + \delta u \\ k(\sigma) &= k(\sigma_0) + \delta k \end{aligned} \tag{10}$$

Substituting (10) into the Helmholtz equation (2) and the outgoing boundary conditions (3), and keeping only linear terms in the increments $\delta\sigma$, δu, and δk, we obtain the system:

$$\partial_x\sigma_0\partial_x\delta u + n_0^2 k^2(\sigma_0)\,\delta u = -\partial_x\,\delta\sigma\;\partial_x\,u_0 - 2k(\sigma_0)\,\delta k\,n_0^2\,u_0, \tag{11}$$

$$(\partial_x + ik(\sigma_0))\;\delta u = -i\,\delta k\,u_0, \quad x = a \tag{12}$$

$$(\partial_x - ik(\sigma_0))\,\delta u = +i\,\delta k\,u_0, \quad x = b\,. \tag{13}$$

An expression for δk can be found by deriving the compatibility equation for the system (11–13). To derive the compatibility condition, multiply (11) by u_0, integrate by parts and use (a) the equation for u_0, (2), (b) the boundary conditions for u_0 and δu, (c) that $\sigma(a) = \sigma(b) = 1$ and (d) that $\delta\sigma(a) = \delta\sigma(b) = 0$. This yields

$$\delta k = \int_a^b \left[\frac{(\partial_x u_0(x))^2}{2k(\sigma_0)\int_a^b n_0^2u_0^2 + i\left[u_0^2(b) + u_0^2(a)\right]}\right]\delta\sigma(x)\,\mathrm{d}x, \tag{14}$$

whence

$$\frac{\delta k}{\delta\sigma}(\sigma_0) = \frac{(\partial_x u_0(x))^2}{2k(\sigma_0)\int_a^b n_0^2u_0^2 + i\left[u_0^2(b) + u_0^2(a)\right]}. \tag{15}$$

We are interested in increasing the value of $\operatorname{Im} k(\sigma)$ (decreasing $|\operatorname{Im} k(\sigma)|$). Note that, to first order in $\delta\sigma$,

$$\Im\left[k(\sigma)\right] = \operatorname{Im} k(\sigma_0) + \left\langle \Im\left[\frac{\delta k}{\delta\sigma}(\sigma_0)\right], \delta\sigma \right\rangle. \tag{16}$$

Thus a small perturbation, $\delta\sigma$ of σ_0, will increase the value of $\operatorname{Im} k$ most rapidly, provided we choose $\delta\sigma$ to be in the direction of *steepest ascent*:

$$\begin{aligned} \delta\sigma &= \Im\left[\frac{\delta k}{\delta\sigma}(\sigma_0)\right] \\ &= \Im\left[\frac{(\partial_x u_0(x))^2}{2k(\sigma_0)\int_a^b n_0^2u_0^2 + i\left[u_0^2(b) + u_0^2(a)\right]}\right]. \end{aligned} \tag{17}$$

Computation of $\delta k/\delta n$ We now consider variations in k due to changes in $n(x)$, with $\sigma = \sigma_0(x)$ fixed. To compute $\delta k/\delta n$, we expand

$$\begin{aligned} n(x) &= n_0(x) + \delta n(x) \\ u(x;n) &= u_0(x) + \delta u(x) \\ k(n) &= k(n_0) + \delta k. \end{aligned} \tag{18}$$

Proceeding in a manner analogous to the above computation, we obtain

$$\delta k = \int_a^b \left[\frac{-2k^2(n_0)\,n_0(x)\,u_0^2(x)}{2k(n_0)\int_a^b n_0^2u_0^2 + i\left[u_0^2(b) + u_0^2(a)\right]}\right]\delta n(x)\,\mathrm{d}x. \tag{19}$$

Therefore

$$\frac{\delta k}{\delta n}(n_0) = \frac{-2k^2(n_0)\,n_0(x)\,u_0^2(x)}{2k(n_0)\int_a^b n_0^2u_0^2 + i\left[u_0^2(b) + u_0^2(a)\right]},$$

and the direction of steepest ascent for δn is given by

$$\begin{aligned} \delta n &= \Im\left[\frac{\delta k}{\delta n}(n_0)\right] \\ &= \Im\left[\frac{-2k^2(n_0)\,n_0(x)\,u_0^2(x)}{2k(n_0)\int_a^b n_0^2u_0^2 + i\left[u_0^2(b) + u_0^2(a)\right]}\right]. \end{aligned}$$

3.2 Sensitivity analysis and gradient ascent in Σ_N

In this subsection, we restrict the results of the previous section on $\delta k/\delta\sigma$ and $\delta k/\delta n$ to structures (σ, n) in the class Σ_N.

As introduced in Section 2, the structure of a given PC structure is specified by $3N-4$ "design" parameters:

$\mathfrak{x} = (x_2, \ldots, x_{N-1})$ possible points of discontinuity of $\sigma(x), n(x)$

$\mathfrak{s} = (\sigma_2, \ldots, \sigma_N)$ values of $\sigma(x)$ on interval (x_{j-1}, x_j),

$\mathfrak{n} = (n_2, \ldots, n_N)$ values of $n(x)$ on interval (x_{j-1}, x_j).

Given a resonance, $k_{\text{old}} = k(\mathfrak{x}_{\text{old}}, \mathfrak{s}_{\text{old}}, \mathfrak{n}_{\text{old}})$, associated with a structure defined by $(\mathfrak{x}, \mathfrak{s}, \mathfrak{n})_{\text{old}} = (\mathfrak{x}_{\text{old}}, \mathfrak{s}_{\text{old}}, \mathfrak{n}_{\text{old}})$, we obtain an improved structure by deforming the initial structure in the direction of the gradient of the objective functional evaluated at $(\mathfrak{x}, \mathfrak{s}, \mathfrak{n})_{\text{old}}$. Thus, we obtain a new or updated structure as follows:

$$\begin{aligned}(\mathfrak{x}, \mathfrak{s}, \mathfrak{n})_{\text{update}} &= (\mathfrak{x}, \mathfrak{s}, \mathfrak{n})_{\text{old}} + \varepsilon \cdot \ (\nabla \operatorname{Im} k)_{\text{old}} \\ &= (\mathfrak{x}, \mathfrak{s}, \mathfrak{n})_{\text{old}} \\ &\quad + \varepsilon \cdot \left(\nabla_{\mathfrak{x}} \operatorname{Im} k, \nabla_{\mathfrak{s}} \operatorname{Im} k, \nabla_{\mathfrak{n}} \operatorname{Im} k\right)_{\text{old}}.\end{aligned}$$

In this paper, we use the notation ∇k to denote the gradient with respect to all parameters: $\mathfrak{x}$, $\mathfrak{s}$, $\mathfrak{n}$, and $\nabla_{\mathfrak{x}} k$, $\nabla_{\mathfrak{s}} k$, $\nabla_{\mathfrak{n}} k$ to denote gradients with respect to the specified parameters. Equivalently and explicitly,

$$\begin{aligned}\mathfrak{x}_{\text{new}} &= \mathfrak{x}_{\text{old}} + \varepsilon \cdot \left(\frac{\partial}{\partial x_2}, \ldots, \frac{\partial}{\partial x_{N-1}}\right) \operatorname{Im} k \Big|_{(\mathfrak{x}_{\text{old}}, \mathfrak{s}_{\text{old}}, \mathfrak{n}_{\text{old}})} \\ \mathfrak{s}_{\text{new}} &= \mathfrak{s}_{\text{old}} + \varepsilon \cdot \left(\frac{\partial}{\partial \sigma_2}, \ldots, \frac{\partial}{\partial \sigma_N}\right) \operatorname{Im} k \Big|_{(\mathfrak{x}_{\text{old}}, \mathfrak{s}_{\text{old}}, \mathfrak{n}_{\text{old}})} \\ \mathfrak{n}_{\text{new}} &= \mathfrak{n}_{\text{old}} + \varepsilon \cdot \left(\frac{\partial}{\partial n_2}, \ldots, \frac{\partial}{\partial n_N}\right) \operatorname{Im} k \Big|_{(\mathfrak{x}_{\text{old}}, \mathfrak{s}_{\text{old}}, \mathfrak{n}_{\text{old}})}\end{aligned} \tag{20}$$

We discuss the choice of ε later in this section.

The following proposition gives expressions for the partial derivatives of a scattering resonance $k(\mathfrak{x}, \mathfrak{s}, \mathfrak{n})$, with respect to the design parameters:

Proposition 1 *In the above notation, we have the following equations for the partial derivatives of $k(\mathfrak{x}, \mathfrak{s}, \mathfrak{n})$ with respect to the design parameters:*

(1) *Variations in k with respect to the jump locations, $\mathfrak{x} = (x_2, \ldots, x_{N-1})$, for $j = 2, \ldots, N-1$, are given by*

$$\frac{\partial k(\mathfrak{x}, \mathfrak{s}, \mathfrak{n})}{\partial x_j} = \frac{(\sigma_j - \sigma_{j+1})\, \partial_x u(x_j^-) \partial_x u(x_j^+) + (n_{j+1}^2 - n_j^2)\, k^2(\mathfrak{x}, \mathfrak{s}, \mathfrak{n})\, u^2(x_j, \mathfrak{x}, \mathfrak{s}, \mathfrak{n})}{i\left(u^2(a, \mathfrak{x}, \mathfrak{s}, \mathfrak{n}) + u^2(b, \mathfrak{x}, \mathfrak{s}, \mathfrak{n})\right) + 2k(\mathfrak{x}, \mathfrak{s}, \mathfrak{n}) \displaystyle\int_a^b n^2(x, \mathfrak{x}, \mathfrak{s}, \mathfrak{n}) u^2(x, \mathfrak{x}, \mathfrak{s}, \mathfrak{n}) \mathrm{d}x}, \tag{21}$$

(2) *Variations in k with respect to $\mathfrak{s} = (\sigma_2, \ldots, \sigma_N)$ satisfy, for $j = 2, \ldots N$,*

$$\frac{\partial k(\mathfrak{x}, \mathfrak{s}, \mathfrak{n})}{\partial \sigma_j} = \frac{\displaystyle\int_{x_{j-1}}^{x_j} (\partial_x u(x'; \mathfrak{x}, \mathfrak{s}, \mathfrak{n}))^2 \, \mathrm{d}x'}{i\left(u^2(a, \mathfrak{x}, \mathfrak{s}, \mathfrak{n}) + u^2(b, \mathfrak{x}, \mathfrak{s}, \mathfrak{n})\right) + 2k(\mathfrak{x}, \mathfrak{s}, \mathfrak{n}) \displaystyle\int_a^b n^2(x, \mathfrak{x}, \mathfrak{s}, \mathfrak{n}) u^2(x, \mathfrak{x}, \mathfrak{s}, \mathfrak{n}) \mathrm{d}x}. \tag{22}$$

(3) *Variations in k with respect to* $\mathfrak{n} = (n_2, \dots, n_N)$*, for* $j = 2, \dots, N$ *are given by:*

$$\frac{\partial k(\mathfrak{x}, \mathfrak{s}, \mathfrak{n})}{\partial n_j} = \frac{-2k^2(\mathfrak{x}, \mathfrak{s}, \mathfrak{n}) \int_{x_{j-1}}^{x_j} n_j u^2(x', \mathfrak{x}, \mathfrak{s}, \mathfrak{n}) \mathrm{d}x'}{i\left(u^2(a, \mathfrak{x}, \mathfrak{s}, \mathfrak{n}) + u^2(b, \mathfrak{x}, \mathfrak{s}, \mathfrak{n})\right) + 2k(\mathfrak{x}, \mathfrak{s}, \mathfrak{n}) \int_a^b n^2(x, \mathfrak{x}, \mathfrak{s}, \mathfrak{n}) u^2(x, \mathfrak{x}, \mathfrak{s}, \mathfrak{n}) \mathrm{d}x}. \tag{23}$$

Proof To prove (22) and (23), we can apply the formulas from Section 3.1 with specially chosen perturbations of (σ_0, n_0). The proof of (21) requires some more care because $\sigma(x)$ and $\partial_x u(x)$ are possibly discontinuous at $x = x_j$.

Choose $a' < a$ and $b' > b$. Multiply (2) by u, integrate over $[a', b']$, and then integrate by parts. This gives

$$u\partial_x u|_{a'}^{b'} - \int_{a'}^{b'} \sigma(\partial_x u)^2 + \int_{a'}^{b'} k^2 n^2 u^2 = 0. \tag{24}$$

The dependence of the terms in this equation on the design parameter x_j has been suppressed. Denote by $\dot{z}$ the derivative of a function z with respect to x_j. We write the integrals in (24) as the sum of integrals over $[a', x_j)$ and $(x_j, b']$. Note that $\dot{\sigma} = 0, \dot{n} = 0$ for $x \neq x_j$. Differentiation of (24) with respect to x_j yields:

$$\begin{aligned}\frac{\partial}{\partial x_j}\left(u\partial_x u|_{a'}^{b'}\right) - \Bigg[& 2\int_{a'}^{x_j} \sigma \partial_x u \partial_x \dot{u} + 2\int_{x_j}^{b'} \sigma \partial_x u \partial_x \dot{u} \\ & + \sigma_j(\partial_x u(x_j^-))^2 - \sigma_{j+1}(\partial_x u(x_j^+))^2 \Bigg] \\ & + 2\int_{a'}^{b'} (k\dot{k}n^2u^2 + k^2n^2u\dot{u}) \\ & + (k^2 n_j^2 u(x_j)^2 - k^2 n_{j+1}^2 u(x_j)^2) = 0.\end{aligned}$$

After a second integration by parts and using (2), we find

$$\begin{aligned}\frac{\partial}{\partial x_j}\left(u\partial_x u|_{a'}^{b'}\right) - 2\dot{u}\sigma\partial_x u|_{a'}^{b'} + 2\int_{a'}^{b'} k\dot{k}n^2u^2 \\ = \sigma_{j+1}(\partial_x u(x_j^+))^2 - \sigma_j(\partial_x u(x_j^-))^2 + k^2 n_{j+1}^2 u(x_j)^2 \\ - k^2 n_j^2 u(x_j)^2,\end{aligned}$$

where we used the flux condition (4) at x_j. Remembering $\sigma(a') = \sigma(b') = 1$, the outgoing boundary conditions (3), and the derivative of the boundary conditions, the above equation simplifies to

$$\begin{aligned}i\dot{k}(u^2(a') + u^2(b')) + 2\int_{a'}^{b'} k\dot{k}n^2u^2 \\ = (\sigma_j - \sigma_{j+1})\,\partial_x u(x_j^-)\partial_x u(x_j^+) + k^2 n_{j+1}^2 u(x_j)^2 \\ - k^2 n_j^2 u(x_j)^2,\end{aligned}$$

where we use the identity

$$\begin{aligned}\sigma_{j+1}(\partial_x u(x_j^+))^2 - \sigma_j(\partial_x u(x_j^-))^2 \\ = \underbrace{\left(\sigma_{j+1}\partial_x u(x_j^+) - \sigma_j \partial_x u(x_j^-)\right)}_{=0 \text{ by } (4)} \left(\partial_x u(x_j^+) + \partial_x u(x_j^-)\right) \\ + (\sigma_j - \sigma_{j+1})\,\partial_x u(x_j^-)\partial_x u(x_j^+).\end{aligned} \tag{25}$$

Finally, we note using the explicit exponential form of u on $[a', a]$ and $[b, b']$, that the expression in (25) is independent of $a' < a$ and $b' > b$. Letting $a' \uparrow a$ and $b' \downarrow b$, we get the expression in (21).

For expressions (22) and (23), we begin by computing, for structures in Σ_N, variations of a resonance with respect to the design parameters $\mathfrak{x}, \mathfrak{s}, \mathfrak{n}$.

Let $\sigma_0(x), n_0(x)$ denote a structure in Σ_N. Admissible perturbations of (σ_0, n_0) are achieved through variations of the values of σ, $\mathfrak{s}$, and n, $\mathfrak{n}$, on each subinterval. $(\delta\sigma, \delta n)$, the total variations of the coefficient functions, σ and n, due to these two kinds of variations, can therefore be expressed as:

$$\delta\sigma = \sum_{j=2}^{N} \frac{\delta\sigma}{\delta\sigma_j}\,\delta\sigma_j \tag{26}$$

$$\delta n = \sum_{k=j}^{N} \frac{\delta n}{\delta n_j}\,\delta n_j \tag{27}$$

The terms on the right hand side of (26), (27) are computed as follows. Note that general variation of $(\tilde{\sigma}, \tilde{n})$, within Σ_N, is of the form:

$$\sigma_{\alpha,\mu} = \tilde{\sigma} + \sum_{j=2}^{N} (\sigma_j + \mu\delta\sigma_j)\ \chi_{[x_{j-1},x_j]},$$

$$n_{\alpha,\mu} = \tilde{n} + \sum_{j=2}^{N} (n_j + \mu\delta n_j)\ \chi_{[x_{j-1},x_j]},$$

where $\chi_{[a,b]}(x)$ denotes the characteristic function of the interval $[a, b]$. Thus,

$$\frac{\delta\sigma}{\delta\sigma_j}\cdot\delta\sigma_j = \frac{\mathrm{d}}{\mathrm{d}\mu}\bigg|_{\mu=0} (\sigma_j + \mu\delta\sigma_j)\ \chi_{[x_{j-1},x_j]} = \chi_{[x_{j-1},x_j]}\cdot\delta\sigma_j \tag{28}$$

$$\frac{\delta n}{\delta n_j}\cdot\delta n_j = \frac{\mathrm{d}}{\mathrm{d}\mu}\bigg|_{\mu=0} (n_j + \mu\delta n_j)\ \chi_{[x_{j-1},x_j]} = \chi_{[x_{j-1},x_j]}\cdot\delta n_j. \tag{29}$$

To prove (22) and (23), for each fixed $j \in \{2, \ldots, N-1\}$, consider the perturbation $\sigma_j \to \sigma_j + \delta\sigma$, respectively, $n_j \to n_j + \delta n_j$, with other parameters held unchanged. Then, by (26–28) and (29), we have

$$\delta\sigma = \chi_{[x_{j-1},x_j]},\quad \delta n = \chi_{[x_{j-1},x_j]}$$

Substitution into (14) and (19) yields the expression (21) for $\partial k/\partial\sigma_j$ and $\partial k/\partial n_j$. □

3.3 Gradient ascent algorithm in Σ_N

Using Proposition 1, we can now compute an updated structure and *approximate corresponding resonance* from the old structure:

$$(\mathfrak{r}, \mathfrak{s}, \mathfrak{n})_{\text{update}} = (\mathfrak{r}, \mathfrak{s}, \mathfrak{n})_{\text{old}} + \varepsilon\cdot \operatorname{Im}\nabla k_{\text{old}} \tag{30}$$

$$k_{\text{approx,update}} = k_{\text{old}} + \varepsilon\cdot(\nabla k_{\text{old}}, \operatorname{Im}\nabla k_{\text{old}})\,; \tag{31}$$

see (20).

The parameter, ε, is carefully chosen so to ensure convergence of the Newton method resonance finder with $k_{\text{approx,update}}$ as initial guess, see Section 4.2. To achieve this, we control the relative distance:

$$p = \left|\frac{k_{\text{approx,update}} - k}{k}\right|.$$

If p is fixed as control parameter for the step length, then one finds

$$\varepsilon = p\cdot\left|\frac{k}{(\nabla k, \operatorname{Im}\nabla k)}\right|.$$

Algorithm 1 Steepest Ascent

Input: k_0 start guess, $(\mathfrak{r}, \mathfrak{s}, \mathfrak{n})_0$ start structure, p control parameter, *eps* accuracy for Newton's method, M number of steepest descent steps.
Output: $(\mathfrak{r}, \mathfrak{s}, \mathfrak{n})_{\text{opt}}$ optimized structure, k_{opt} optimized resonance.

1 $k_{\text{opt}} \leftarrow$ result of Newton's method with accuracy *eps* and initial guess $k = k_0$ for the initial structure $(\mathfrak{r}, \mathfrak{s}, \mathfrak{n})_0$.
2 For *count* $= 1, \ldots, M$
3 Let $\varepsilon \leftarrow p\cdot\left|\frac{k_{\text{opt}}}{(\nabla k_{\text{opt}}), \operatorname{Im}\nabla k_{\text{opt}})}\right|$, where ∇k_{opt} is computed by Proposition (1) with k_{opt}
4 $k_{\text{approx,update}} \leftarrow k_{\text{opt}} + \varepsilon\cdot(\nabla k_{\text{opt}}, \operatorname{Im}\nabla k_{\text{opt}})$
5 $(\mathfrak{r}, \mathfrak{s}, \mathfrak{n})_{\text{opt}} \leftarrow (\mathfrak{r}, \mathfrak{s}, \mathfrak{n})_{\text{opt}} + \varepsilon\cdot\operatorname{Im}\nabla k_{\text{opt}}$
6 $k_{\text{opt}} \leftarrow$ result of Newton's method with accuracy *eps* and initial guess $k_{\text{approx,update}}$ for the structure $(\mathfrak{r}, \mathfrak{s}, \mathfrak{n})_{\text{opt}}$.
7 end for

4 Numerical computation of scattering resonances

In this section, we focus on the numerical determination of scattering resonances of structures in the class Σ_N. Then, we outline a gradient ascent method, which finds locally optimal structures of class Σ_N. For our numerical ascent scheme, we need three different ingredients. First, we need a discretization of the scattering resonance problem (**SRP**) (2, 3). Second, we need a numerical routine to solve the discretized problem. The starting point for this latter step is typically an approximate solution of the discretized problem and a routine that *corrects* this guess. Finally, we perform a gradient ascent step, which provides an approximate improved structure.

We will present two different ways for the discretization of (2). The first approach (see Section 4.1) exploits the property that, for piecewise constant one-dimensional structures, the equation is exactly solvable on each subinterval. The solution is determined by matching conditions for the functions and fluxes at the subinterval endpoints. The second approach (see Section 4.3) uses a finite difference discretization for (2). The corrector routine for both methods is a Newton root finder (Section 4.2), which is adapted for the particular discretization. The gradient ascent step is the same for both methods and is based on Proposition 1.

4.1 Matching method

We introduce the following simplifying notation:

$$r_j := \frac{n_j}{\sqrt{\sigma_j}}, \quad j = 1, \ldots, N+1. \tag{32}$$

The solution of (2) is given by

$$u(x) = \begin{cases} c_1 e^{-ikx} & : \quad x < a \\ c_{2j} e^{ir_{j+1}kx} + c_{2j+1} e^{-ir_{j+1}kx} & : \quad x_j < x < x_{j+1},\ j = 1, \ldots, N-1 \\ c_{2N} e^{ikx} & : \quad b < x \end{cases}, \tag{33}$$

where the complex coefficients $c_1, \ldots, c_{2N}$ are determined from the conditions that $u(x)$ be continuous on $\mathbb{R}$ and such that the flux continuity relations (4) are satisfied at the jump locations, x_j.

Writing down these matching conditions gives the following set of equations at x_1:

$$\begin{aligned} c_1 e^{-ikx_1} &= c_2 e^{ir_2 kx_1} + c_3 e^{-ir_2 kx_1} \\ -c_1 e^{-ikx_1} &= r_2\left(c_2 e^{ir_2 kx_1} - c_3 e^{-ir_2 kx_1}\right), \end{aligned}$$

at x_j for $j = 2, \ldots, N-1$:

$$\begin{aligned} c_{2j-2} e^{ir_j kx_j} + c_{2j-1} e^{-ir_j kx_j} &= c_{2j} e^{ir_{j+1} kx_j} + c_{2j+1} e^{-ir_{j+1} kx_j} \\ r_j(c_{2j-2} e^{ir_j kx_j} - c_{2j-1} e^{-ir_j kx_j}) &= r_{j+1}\big(c_{2j} e^{ir_{j+1} kx_j} \\ &\quad - c_{2j+1} e^{-ir_{j+1} kx_j}\big), \end{aligned}$$

at x_N:

$$\begin{aligned} c_{2N-2} e^{ir_N kx_N} + c_{2N-1} e^{-ir_N kx_N} &= c_{2N} e^{ikx_N} \\ r_N(c_{2N-2} e^{ir_N kx_N} - c_{2N-1} e^{-ir_N kx_N}) &= c_{2N} e^{ikx_N}. \end{aligned}$$

This is a linear system of $2N$ equations of the form

$$A(k)c = 0.$$

The matrix $A(k) \in \mathbb{C}^{2N \times 2N}$ depends nonlinearly on the wavenumber k and has a narrow band structure, which will be exploited in the numerical scheme. The mode $u(x)$ is recovered from k and the amplitude vector c.

To impose that the solution we find is nontrivial, we impose a normalization condition on the vector c; for example, one can set the amplitude c_1 of the scattered part at the left end to 1. Thus, one arrives at the following nonlinear discretized problem:

$$F(k, c) := \begin{pmatrix} A(k) \cdot c \\ e_1^T c - 1 \end{pmatrix} = 0. \tag{34}$$

This is a system of $2N+1$ nonlinear equations in the $2N+1$ unknowns $k, c_1, \ldots, c_{2N}$. Of course, one could reduce this system by one dimension by eliminating the fixed c_1, but for notational ease, (34) will be used in the following.

Equation (34) can be solved by any kind of nonlinear solver. We use Newton's method, which is outlined in the next subsection.

4.2 Newton's method

For a given structure in Σ_N, with resonance energy k and mode amplitude vector c, we typically have an approximate or guessed resonance k^0 and amplitude vector c^0 . If $\|(k^0, c^0) - (k, c)\|$ is sufficiently small, then Newton's method applied to (34) guarantees convergence. With a good initial guess, Newton's method converges quadratically, and few iteration steps are necessary. Moreover, the error in the computation of k and c (and thus of $u(x)$) can be estimated by Newton's method.

Newton iteration, applied to (34), reads

$$DF(k^j, c^j)\begin{pmatrix} c^{j+1} - c^j \\ k^{j+1} - k^j \end{pmatrix} = -F(k^j, c^j),$$

where

$$DF(k, c) = \begin{pmatrix} A(k) & A'(k)c \\ e_1^T & 0 \end{pmatrix}$$

is the Jacobian of $F(k, c)$. Written out, this equation yields

$$A(k^j)c^{j+1} + (k^{j+1} - k^j) \cdot A'(k^j)c^j = 0$$
$$e_1^T c^{j+1} = 1,$$

which is formulated in the *Newton step*

$$\text{(NA)} \qquad \begin{aligned} A(k^j)y^{j+1} &:= A'(k^j)c^j, \\ c^{j+1} &:= \frac{y^{j+1}}{e_1^T y^{j+1}} \\ k^{j+1} &:= k^j - \frac{1}{e_1^T y^{j+1}}. \end{aligned}$$

Remarks:

- The matrices $A(k)$ and $A'(k)$ are explicitly known, and their computation can easily be implemented.
- As $A(k)$ is sparse, one can find y^{j+1} efficiently.
- The matrices $A(k)$ and $A'(k)$ can be stored with $O(8N)$ memory.

4.3 Finite difference discretization of resonance problem

In this subsection, we present a second approach to computation of scattering resonances, based on a finite difference solution of the scattering resonance problem. For simplicity, we take $n(x) \equiv 1$; the required modifications for general $n(x)$ are straightforward.

Let $U(x; k)$ and $V(x; k)$ denote solutions of (2) which are outgoing at $x = a$, respectively, $x = b$:

$$(\partial_x + ik)\, U(x; k)\,|_{x=a} = 0, \quad U(a; k) = 1 \tag{35}$$

$$(\partial_x - ik)\, V(x; k)\,|_{x=b} = 0, \quad V(b; k) = 1. \tag{36}$$

For typical values of k, $U(x; k)$ and $V(x; k)$ are linearly independent. Let $W(k)$ denote the *Wronskian* of U and V:

$$W(k) = V(x; k)\sigma(x)\partial_x U(x; k) - U(x; k)\sigma(x)\partial_x V(x; k). \tag{37}$$

$W(k)$ is independent of x. U and V are linearly dependent if and only if $W(k) = 0$. In this case, U and V are proportional. Thus, if $W(k_*) = 0$, then $U(x; k)$ is outgoing at $x = a$ and $x = b$, and the pair $(U(x; k_*), k_*)$ is a scattering resonance. As remarked in Section 1, scattering resonance energies (zeros of $W(k)$) are in the lower half plane, $\operatorname{Im} k < 0$.

We now turn to a finite difference implementation. Partition $[a, b]$ into N intervals of length $\Delta x = (b - a)/N$. We introduce a scheme for approximating $u(x)$ at discrete grid-points

$$u_j = u(y_j), \quad y_j = (j - 1)\Delta x, \quad j = 1, \ldots, N. \tag{38}$$

We use the symmetric discretization of (2) is

$$\frac{\sigma_{j+\frac{1}{2}}(u_{j+1} - u_j)}{(\Delta x)^2} - \frac{\sigma_{j-\frac{1}{2}}(u_j - u_{j-1})}{(\Delta x)^2} + k^2 u_j = 0 \tag{39}$$

where $y_j = a + (j - 1)\Delta x$. This discretization respects the continuity of flux condition (4). The points of discontinuity of $\sigma(x)$ are chosen to be grid points. The scheme uses values of σ at staggered points $y_{j+\frac{1}{2}}$, where $\sigma\left(y_j + \frac{1}{2}\right) = \sigma_{j+\frac{1}{2}}$.

We shall use the scheme (39) to construct out fundamental set $\{U(x; k), V(x; k)\}$. To do so, we require appropriate discretizations of the outgoing conditions (35) and (36). These discrete outgoing conditions at $x = a$ and $x = b$ are derived as follows.

At the ends of the domain, the equation becomes

$$\frac{u_{j+1} - 2u_j + u_{j-1}}{(\Delta x)^2} + k^2 u_j = 0. \tag{40}$$

This constant coefficient difference equation has, for $k\Delta x$ sufficiently small, oscillatory exponential solutions

$$u_j = A\,\xi^j + B\,\xi^{-j}, \tag{41}$$

where ξ is the root of the quadratic equation $z^2 - \left(2 - (k\Delta x)^2\right)z + 1 = 0$ corresponding to the choice of positive square root:

$$\xi = \frac{\left(2 - (k\Delta x)^2\right) + i\sqrt{4 - \left(2 - (k\Delta x)^2\right)^2}}{2}. \tag{42}$$

The discrete solution u_j is outgoing to the right provided $B = 0$. Therefore, the discrete boundary condition for a solution which is outgoing to the right $x = x_N = b$ is

$$V_{j+1} = \xi\, V_j, \quad j = N - 1. \tag{43}$$

We also have from (36) the normalization $V_N = 1$, which together with (43) gives

$$V_{N-1} = \xi^{-1}. \tag{44}$$

Analogously, the discrete outgoing to the left condition at $x = a$ is

$$U_j = \xi^{-1}\, U_{j-1}, \quad j = 2, \tag{45}$$

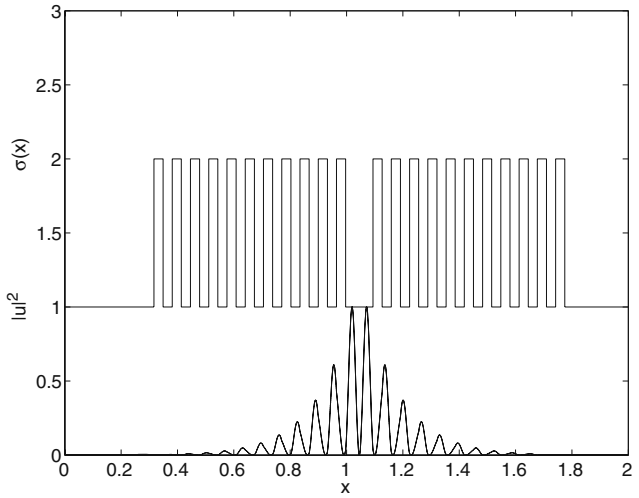

Fig. 2 The initial structure for all three scenarios. It consists of 22 barriers and a *missing barrier* in the middle. The outgoing wave conditions are imposed on the left resp. right end of the structure. *Below* is the resonance mode (modulus squared) of the chosen initial resonance

which together with the normalization from (35), $U_1 = 1$, gives

$$U_2 = \xi^{-1}. \tag{46}$$

To construct the approximation to $U(x;k)$, we obtain U_2 from (46) and use the expression for U_{j+1} obtained from (39) to propagate this value forward to obtain U_j, $j = 3, \ldots, N$. Similarly, to construct the approximation to $V(x;k)$ we obtain V_{N-1} from (44) and then use the expression for V_{j-1}, obtained from (39) to back-propagate the solution obtaining V_j for $j = N-2, \ldots, 1$.

Finally, we require a discretized version of the Wronskian, $W(k)$. The discrete Wronskian is given by:

$$\mathcal{W}(k) = \sigma_{j+\frac{1}{2}} \left[\frac{U_j(k)(V_{j+1}(k) - V_j(k)) - V_j(k)(U_{j+1}(k) - U_j(k))}{\Delta x}\right], \tag{47}$$

which is independent of j.

Scattering resonance frequencies of our discrete approximation (39, 43, 45) are values of k for which the discrete Wronskian is zero,

$$\mathcal{W}(k) = 0. \tag{48}$$

In this implementation, the numerical scheme for finding a scattering resonance of a fixed structure, $(\sigma(x), n(x))$, starts with an approximate scattering resonance $k_{res,0}$ (an approximate root of (48)) and improves it by Newton iteration:

$$k_{\mathrm{res},r+1} = k_{\mathrm{res},r} - \frac{\mathcal{W}(k_{\mathrm{res},r})}{\partial_k \mathcal{W}(k_{\mathrm{res},r})}, \quad r = 0, 1, \ldots \tag{49}$$

Remark 2 There are serious issues of instability in searching for approximate zeros of $W(k)$ by seeking zeros of the discrete Wronskian, $\mathcal{W}(k)$, constructed from the numerical approximations U_j and V_j. Though in theory a constant in j, the numerically computed Wronskian, $\mathcal{W}^{\mathrm{computed}}(k; y_j)$, oscillates with j due to roundoff error. This can be overcome by applying Newton's method to an *averaged* Wronskian: $\mathcal{W}(k) = N^{-1} \sum_{j=1}^{N} \mathcal{W}^{\mathrm{computed}}(k; y_j)$.

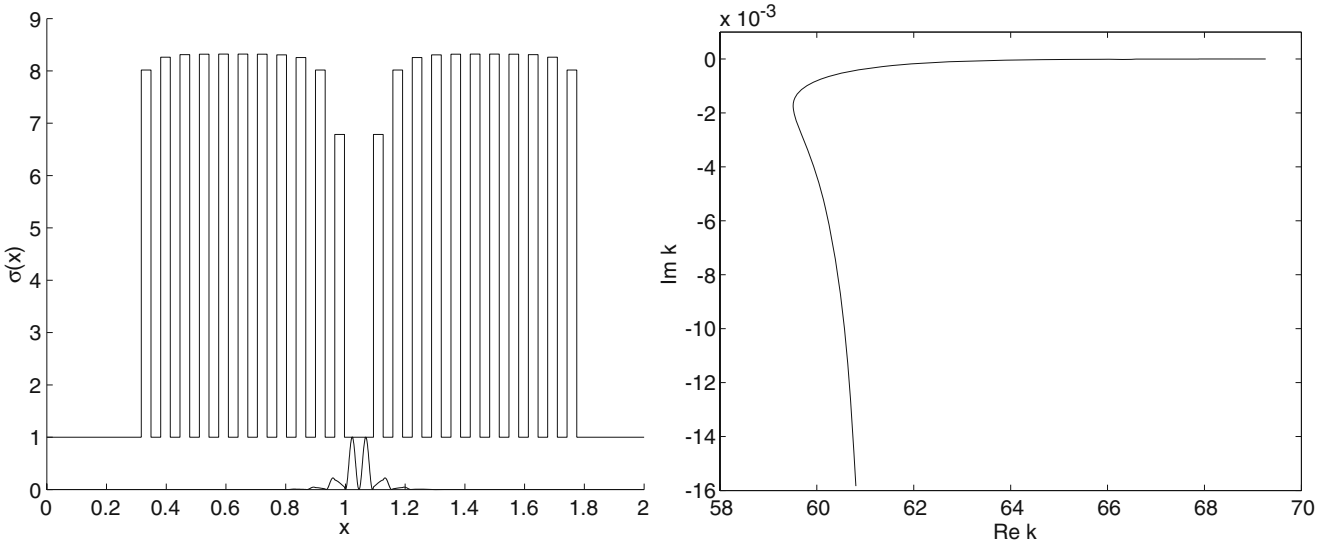

Fig. 3 *Left* optimal structure for Problem Opt together with optimized resonance mode. The optimized mode is more concentrated within the defect than the initial mode. *Right* the path of the resonance during optimization

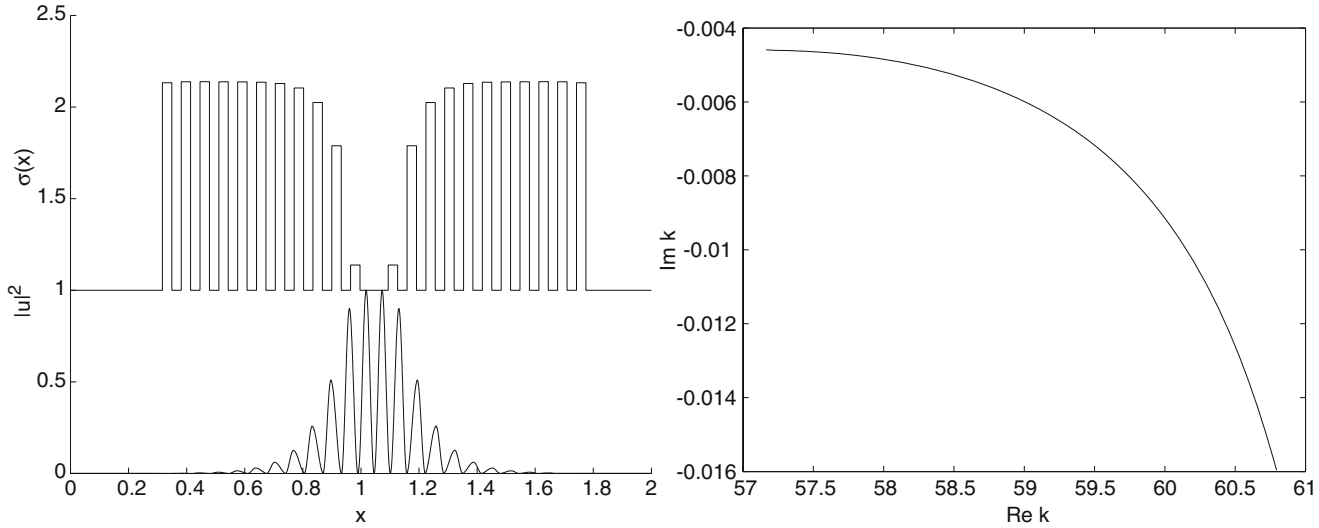

Fig. 4 *Left* optimal structure for Problem $\mathrm{Opt}_{\mathrm{area}}$ together with optimized resonance mode. *Right* the path of the resonance during optimization for scenario $\mathrm{Opt}_{\mathrm{area}}$

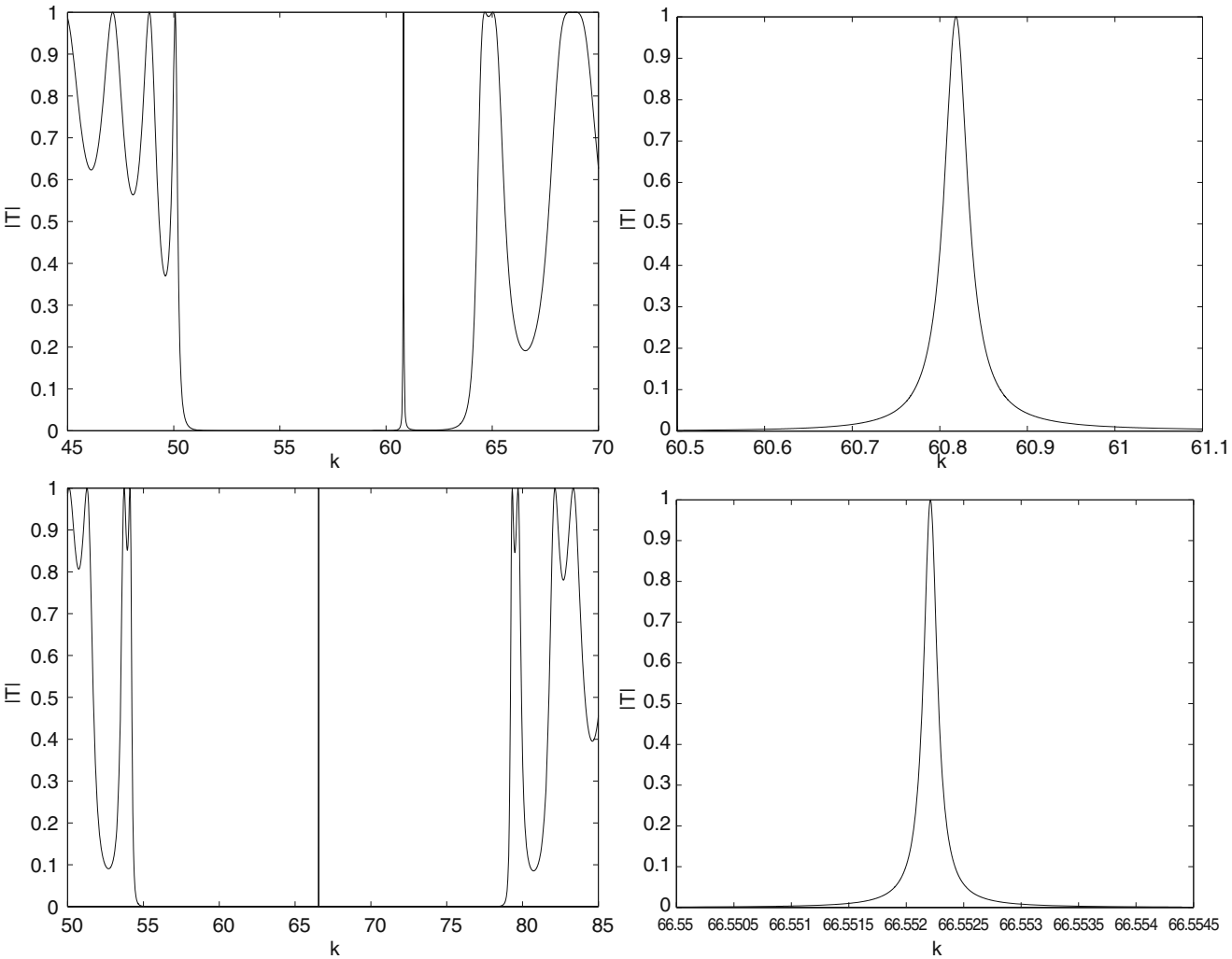

Fig. 5 Transmission diagram for the initial structure (*top*) and the optimized structure (*bottom*) of problem $\mathrm{Opt}_{\mathrm{max}}$. The band-gap shifted during the optimization, and the resonance is sitting nearly in the middle of the band-gap of the optimized structure. To the right zoom of the resonance peak in each case. After successful optimization, the resonance peak gets very sharp

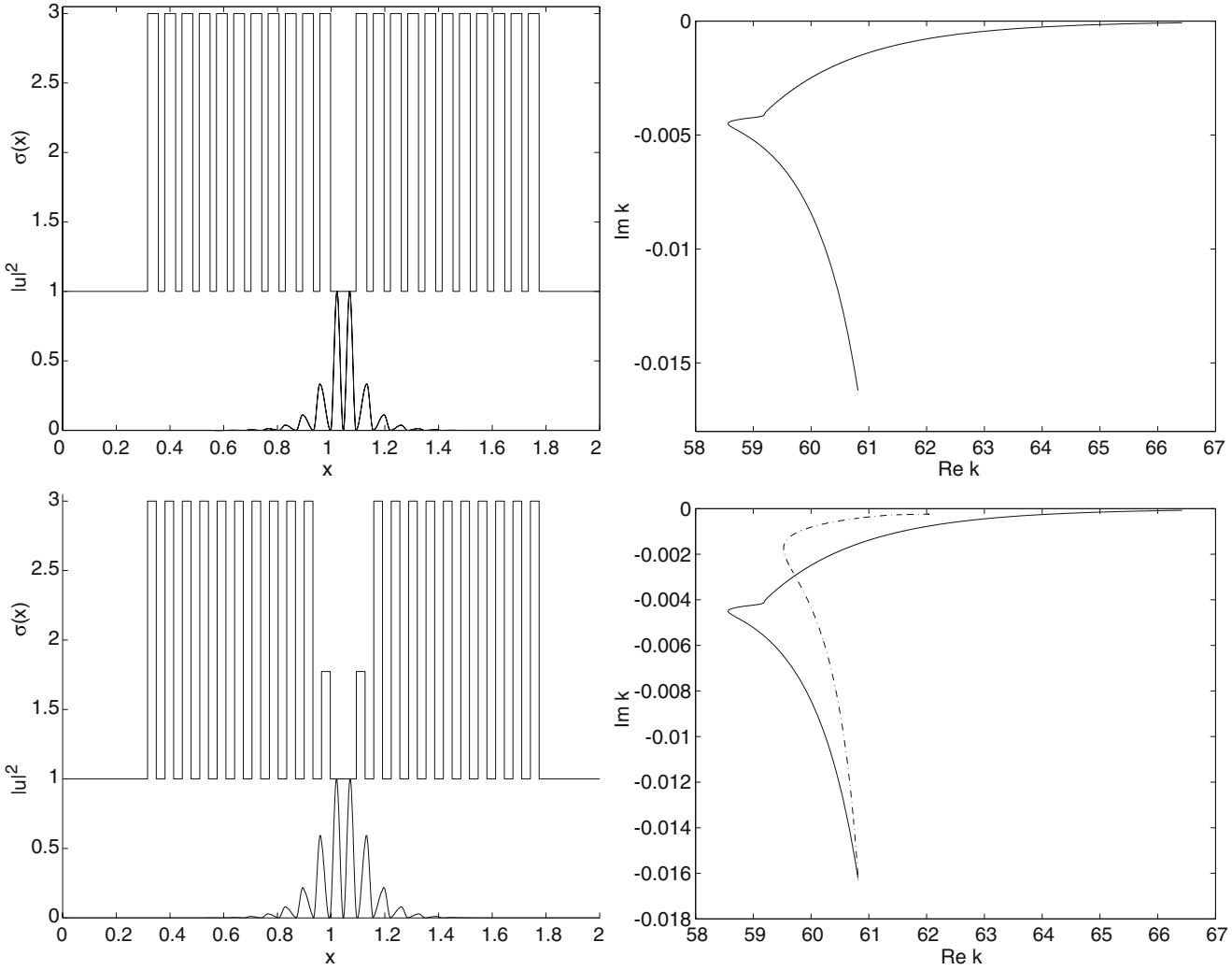

Fig. 6 *Top left* optimal structure for Problem Opt_{max} together with optimized resonance mode. *Top right* the path of the resonance during optimization for problem Opt_{max}. *Bottom left* optimized structure with fixed jump positions. *Bottom right* path of the resonances during optimization, *solid line* with varying jumps, *scattered line* with fixed jumps

5 Numerical results

We performed numerical gradient ascent for the three optimization problems Opt, Opt_{area}, and Opt_{max}. For all simulations, we use the same initial truncated periodic structure with a defect. Both methods, matching and finite difference, were used to solve for and optimize scattering resonances and gave consistent results. We performed our most extensive investigations using the matching approach, due to its greater efficiency.

The initial structure we used is shown in Fig. 2: $\sigma(x)$ is piecewise constant. There is a central defect region of width 3Δ on which $\sigma(x) = 1$. Moving outward from the defect, σ takes on the values $\sigma = 2$ (barriers) and $\sigma = 1$ on alternating intervals of width $\Delta = 0.0324$. This particular example has 22 barriers.

We have chosen $k_0 = 60.8183630665 - 0.0163109133i$ as the initial resonance for all three optimization problems. The associated resonance mode is also plotted in Fig. 2. To find this k_0, an initial approximation is guessed from the value of k at which the transmission diagram has a peak, see Fig. 5—top. Starting with this real value of k as an initial guess, Newton iteration was then used to find an accurate k_0.

For the problems Opt and Opt_{area}, we kept the jump positions fixed during the optimization, whereas for problem Opt_{max}, we also allowed the jump positions to vary.

5.1 Problem Opt

Gradient ascent was applied to the above structure and yielded a (local) optimal resonance $k_{\text{opt}} =$

$69.2633131254 - 0.0000004471i$. The Q-factor is four orders of magnitude larger than that of the initial resonance. We stopped the ascent iteration with $\|\nabla \mathrm{Im}\, k_{\mathrm{opt}}\| = 4.17053 \cdot 10^{-7}$.

In Fig. 3, the optimal structure and optimal resonance mode are plotted. The path of the resonance during the optimization in the complex plane is also plotted in that figure. Observe the smooth turning point, indicating $\|\nabla Re\, k(\sigma_{\mathrm{tur}})\| = 0$ for a particular structure σ_{tur} visited during optimization.

5.2 Problem $\mathrm{Opt}_{\mathrm{area}}$

Fixing the initial area of σ imposes an additional constraint. The optimal resonance was found to be $k_{\mathrm{area}} = 57.1639554364 - 0.0045894230i$, whose Q-factor is only a single order of magnitude larger than that of the initial structure. The structure and resonance mode are plotted in Fig. 4. Comparing the path of the resonance in Fig. 4 with the path in Problem Opt, one sees that the additional constraint strongly influences the search directions of the ascent method.

5.3 Problem $\mathrm{Opt}_{\mathrm{max}}$

In this study, we constrain the values of $\sigma(x)$ to lie between upper and lower bounds:

$$1 = \sigma_{\min} \leq \sigma \leq \sigma_{\max} = 3.$$

In contrast to the previous simulations, the jump positions can now also vary. The optimal resonance was found to be $k_{\mathrm{opt}} = 66.55233131 - 0.000071246i$, whose Q-factor is three orders of magnitude larger than that of the initial structure. We stopped the ascent iteration after the bounds for σ were reached and $\|\nabla_x \mathrm{Im}\, k_{\mathrm{opt}}\| = 1.69 \cdot 10^{-7}$.

We also ran the simulation with fixed jumps to compare the optimal structures and resonances. For this case, the optimal resonance was found to be $k_{\mathrm{opt}} = 62.0211038345 - 0.0002390987i$.

In Fig. 5, the transmission diagram of the initial structure (top panel) together with the optimized structure of Problem $\mathrm{Opt}_{\mathrm{max}}$ (bottom panel) is shown. As expected, the peak corresponding to the optimized resonance k_{opt} is much sharper than the peak belonging to k_0. The band-gap shifted during the optimization, and the resonance peak of the optimized structure is nearly in the middle of the band-gap.

We note that, when allowing, in addition to the values of σ, the locations of possible jumps, $\{x_j\}_{j=2}^{N-1}$, to vary, that the optimal structure is found to be one whose parameter values achieve the bounds $\sigma_{\min}$ and $\sigma_{\max}$, see Fig. 6. We have also observed, in our optimization, the emergence of structures, similar to *Bragg resonators*, whose intervals of constant σ are multiples of one quarter of the wavelength in the local material. These properties are currently under investigation.

References

Burger M, Osher S, Yablonovitch E (2004) Inverse problem techniques for the design of photonic crystals. IEICE Trans Electron 87:258–265

Cox SJ, Dobson DC (1999) Maximizing band gaps in two-dimensional photonic crystals. SIAM J Appl Math 59:2108–2120

Cuccagna S (2007) Dispersion for Schrödinger equation with periodic potential in 1D. arxiv:math/0611919v1[math.AP]

Dobson DC, Santosa F (2004) Optimal localization of eigenfunctions in an inhomogeneous medium. SIAM J Appl Math 64:762–774

Figotin A, Klein A (1998) Midgap defect modes in dielectric and acoustic media. SIAM J Appl Math 58:1748–1773

Geremia JM, Williams J, Mabuchi H (2002) Inverse-problem approach to designing phononic crystals for cavity QED experiments. Phys Rev E 66:066606

Joannopoulos JD, Meade RD, Winn JN (1995) Photonic crystal: molding the flow of light. Princeton Univ. Press, Princeton, NJ

Kao C-Y, Santosa F (2007) Maximization of the quality factor of an optical resonator. doi:10.1016/j.wavemoti.2007.07.012

Kao CY, Osher S, Yablonovich E (2005) Maximizing band gaps in two-dimensional photonic crystals by using level set methods. Appl Phys B Lasers Optics 81:235–244

Korotyaev E (1997) The propagation of waves in periodic media at large time. Asymptot Anal 15:1–24

Lipton RP, Shipman SP, Venakides S (2003) Optimization of resonances of photonic crystal slabs. In: Proceedings SPIE, vol 5184, pp 168–177

Osher S, Santosa F (2001) Level set methods for optimization problems involving geometry and constraints—I. Frequencies of two-density inhomogeneous drum. J Comp Phys 171:272–288

Pironneau O (1984) Optimal shape design for elliptic systems. Springer

Ramdani K, Shipman S (2007) Transmission through a thick periodic slab. Math Models Methods Appl Sci

Sigmund O, Jensen JS (2003) Systematic design of phononic band-gap materials and structures by topology optimization. Phil Trans R Soc London A 361:1001–1019

Tang S-H, Zworski M (2000) Resonance expansions of scattered waves. Commun Pure Appl Math 53:1305–1334